J Nanostruct 13(2): 567-575, Spring 2023

RESEARCH PAPER

The Investigating the Performance of Diffraction Rings Formation in Fe_2O_3 Nano-Fragments at Different Wavelengths

*H. M. Sobhi *, A. B. Sharba, and J. M. Jassim*

Department of Laser Physics, College of Science for Women, University of Babylon- 51002, Babylon, Iraq

ARTICLE INFO

Article History:
Received 13 January 2023
Accepted 25 March 2023
Published 01 April 2023

Keywords:
Amorphous Fe_2O_3 Nano-fragments
Linear and nonlinear properties
Spatial self-phase modulation technique

ABSTRACT

In this work, the structural and optical properties of Fe_2O_3 Nano-fragments suspension in ethanol were studied in detail. The optical study includes characterizing the nonlinear response of the particles by using the spatial self-phase modulation (SSPM) technique at several wavelengths (405, 532, and 650 nm). The structure and the size distribution of the collides were studied by performing X-ray diffraction (XRD) analysis, the Fourier Transformation Infrared spectroscopy (FT-IR), and Transmission Electron Microscopy (TEM) measurements. As a possible application, the potential of configuring an optical switch was also verified. The experimental results indicate that, for the amorphous Fe_2O_3 Nano-fragments with sizes ranging between 5-50 nm, the value of the nonlinear refractive index of Fe_2O_3 particles is about (0.8×10^{-11}-2.73×10^{-11} m^2/W) at 405nm. In addition, a pump beam at this wavelength can control any other probe beam at different wavelengths, regarding less the intensity of the probe beam. At wavelengths 532 nm and 650 nm diffraction rings cannot be formed within the light intensity used in this work (exceeding 25 MW/m^2). The results of this study reveal the possibility of using these particles in optoelectronics and photonics applications.

How to cite this article
Sobhi H. M. , Sharba A. B., and Jassim J. M. The Investigating the Performance of Diffraction Rings Formation in Fe_2O_3 Nano-Fragments at Different Wavelengths. J Nanostruct, 2023; 13(2):567-575. DOI: 10.22052/JNS.2023.02.027

INTRODUCTION

The nonlinear optics is of great interest in the field of optoelectronic applications, including communications, signal processing, data storage, and optical switches [1-4]. Therefore, the need for nonlinear materials is necessary to improve the performance of optical devices operating in many fields [5,6]. In addition, technological developments in optoelectronics have contributed to increasing the demand for nonlinear materials that are used in optical limiters, optical switches, and other essential applications [7-11].

Nano-scale materials are important kinds of materials that are widely used in the field of nonlinear optics. They have many important applications in optoelectronics, medicine, sensor technology, biological labeling, treatment of some types of cancers, and diodes [12-19]. In particular, metal oxides, especially in amorphous form, have attained great interest for their important potential applications in several fields, e.g. [14-17]. The intrinsic optical isotropy is one of the most important characteristics of amorphous material. In addition, the disordered arrangement of material imparts important features and overcomes many limitations that are intrinsic in crystalline material [14,17]. Iron oxides (Fe_3O_4, αFe_2O_3, γFe_2O_3 ... etc.) are important Nano-

* Corresponding Author Email: *hala.subhai.gsci49@student.uobabylon.edu.iq*

materials that are used in many biological and geological processes [13,18-20]. The properties of many iron compounds, including the linear and nonlinear optical properties, have been widely studied, e.g. see [2, 5, 21-25].

In the field of nonlinear optics, there are many techniques for detecting nonlinear optical properties. One of those commonly used techniques is the Z-scan method, discovered in 1989 by Sheik-Bahaa. It was used to determine the refractive index and the absorption nonlinearity of third-order nonlinear optical materials [26,27]. The spatial self-phase modulation (SSPM) technique is another simple and efficient method for characterizing the nonlinear refraction of material. It uses self-diffraction rings that are formed in the far field to determine the nonlinear refractive index and the third order nonlinear susceptibility $\chi^{(3)}$ of the studied materials [28, 29]. Recently, SSPM technique is widely employed to characterize the nonlinearity of many 2D Nano-materials, e.g. [2, 3, 5, 7]. There are many other techniques for detecting nonlinear properties, including (Non-linear imaging technique, and the D4 method inside a 4f-Z-Scan system) [30].

In this work, structural, linear, and nonlinear optical properties of amorphous Fe_2O_3 Nano-fragments suspension in ethanol were studied in detail. The structural investigation includes performing TEM, FT-IR, and XRD measurements. The nonlinear optical properties were studied by using SSPM technology with wavelengths (405, 532, and 650 nm). This study also presents the effect of concentration and light intensity on the nonlinear refractive index of the Fe_2O_3 suspensions. The performance of all-optical switch was also investigated.

THEORETICAL BASIS

The total refractive index of a medium is dependent on the incident light intensity with the formula [6]

$$n = n_o + n_2 I \tag{1}$$

where : the linear refractive index, : the nonlinear refractive index, and : the intensity of the laser beam incident on the sample.

The third-order nonlinear susceptibility can be given as [7]

$$\chi^{(3)}_{Total} = \frac{c\lambda n_o}{2.4 \times 10^4 \pi^2 L_{eff}} \frac{dN}{dI} \tag{2}$$

with:

$$L_{eff} = z_o tan^{-1}\left(\frac{z}{z_o}\right)\Big|_{L_1}^{L_2} \tag{3}$$

where: is the speed of light in vacuum, is the wavelength, is the number of rings, is the Rayleigh range, is the propagation length, and are the distances from the front and the back faces of the sample cell to the focal plane of the beam.

The nonlinear refractive index can be found by using the SSPM technique. The SSPM refers to the phenomenon of the interaction of a laser beam passing through a medium with the same medium as it modifies the phase of the same beam. The origin of this phenomenon lies in the ability of the laser beam to cause appreciable changes in the refractive index of the medium in a way that is dependent on the intensity of the laser beam. These changes lead to modify the phase of the laser beam, which leads to the appearance of diffraction rings at the far field. The spatial distribution of the laser beam is variable in the cross-section; therefore, the phase change has a spatial cross-section dependence, which distorts the wave front of the beam. The spatial phase change is responsible for the well-known nonlinear optical phenomena such as self-focusing and self-defocusing of the laser beams. If the phase change is large enough, it can lead to the formation of a number of concentric diffraction rings at the far field [31]. In such a case, the nonlinear refractive index can be concluded from the number of rings formed using the relationship below [3]

$$n_2 = (N + \delta\ ) \frac{\lambda\, \alpha\, C}{0.868\, n_0\, I_0 \left(1 - e^{\frac{\alpha c L}{0.434}}\right)} \tag{4}$$

where, is the attenuation length, is the concentration of the suspension. : is the extinction coefficient, and: is the relative error.

MATERIALS AND METHODS

The Fe_2O_3 Nano-fragments used in this work have been purchased from (PlasmaChem) in the form of Nano-particles suspension in water. To examine the properties of these materials in ethanol, the material was dried and then placed in ethanol with different weights. After that, the samples have been exposed to ultrasonic waves using an ultrasonic device.

The absorption spectrum of Fe_2O_3 suspension

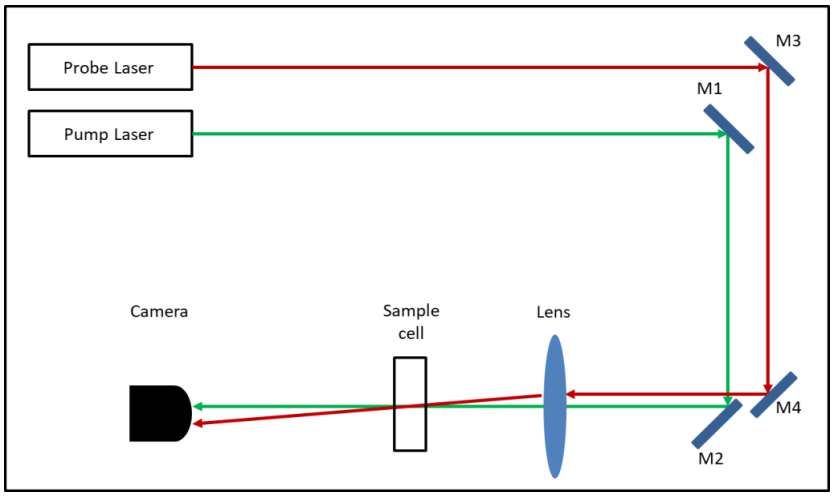

Fig. 1. Experimental setup of the SSPM technique. M1-4 are high reflecting mirrors.

was measured within the range (190-900nm) by using a CECIL CE 7200 UV-Visible spectrophotometer. To identify the material, an FTIR examination of the samples was carried out using a Fourier transform infrared spectrometer equipped by BRUKER. The crystalline structure of the particle was examined by performing an XRD measurement. The shape and the size distribution of the suspension were investigated by implementing TEM measurements.

As for the detection of the nonlinear properties of the samples, the spatial self-phase modulation (SSPM) technique was used. Fig. 1 shows the experimental setup of this technique.

For the SSPM characterization, continuous wave diode lasers at wavelengths (405, 532, and 650 nm) were used with power ranging from 25 to 90 mW. The laser power was controlled by using optical density filters. The laser beam is directed by using two highly reflecting mirrors and then focused by using a lens with a focal length of 10 cm. The sample under examination was placed in a cell of 1 cm thickness. This cell is placed at a distance of (15 mm) before the focal plane of the lens. The formed rings were pictured by using a charged coupled device (CCD). The time evolution of the formed diffraction rings was recorded with a video camera that has a speed of 60 frame per second.

To check the feasibility of the optical switch, an 0.5 mW He-Ne laser was used as a probe beam. This beam was directed parallel to the pump beam by using two mirrors. Then, this beam is focused by the same lens used to focus the pump as shown in Fig. 1. The time evolution of the pump and probe rings was also filmed using a video camera.

RESULTS AND DISCUSSION

Fe_2O_3 Nano-fragments in ethanol have linear absorption in the ultraviolet region. The highest absorption is at wavelengths that range from (210 nm) to (256 nm), as shown in Fig. 2.

The figure shows the absorption spectra of different concentrations of the Fe_2O_3 nano-material. As the wavelength increases, the absorbance decreases gradually until it becomes relatively low in the visible region. It becomes almost flat in the infrared range.

To examine the bonding structure of the studied material, an FT-IR test was conducted. Fig. 3 presents the transmission spectrum of the studied sample. The peak at 3606 cm^{-1} is well known to be for the O-H stretching and those around

1600 cm^{-1} are for the C=O. The peaks at wavenumbers less than 700 cm^{-1} are for the Fe-O stretching [32].The size and shape of Nano-particles are the key factors that determine the type and strength of the optical response of the particles, especially the nonlinear response. Before drying, the Fe_2O_3 particles in the aqueous solution had spherical shapes. However, the TEM images in Fig. 4 show that the shapes of the Fe_2O_3 particles in ethanol are mostly irregular. They are in the form of fragments of various shapes. This change in shape can be due to the adhesion of iron oxide particles to each other, which leads to the formation of fragments of different shapes. In general, the size of these fragments ranges from 5

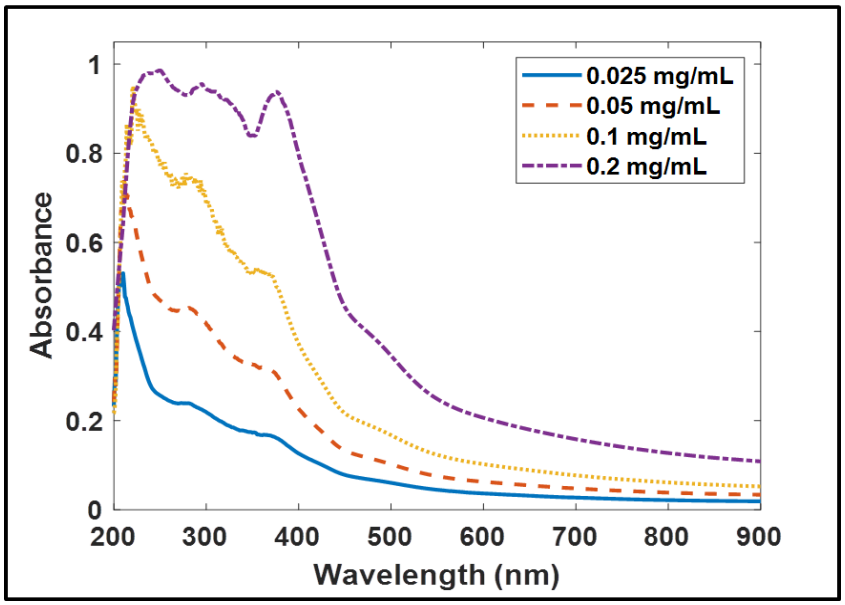

Fig. 3. FT-IR transmission spectrum of Fe_2O_3 Nano-fragments

to 50 nm on average. In addition, it can be observed that these particles suffer from agglomerations. Larger scale images show a high percentage of these particles gathering in the form of relatively large clumps.

The amorphous structure of the Fe_2O_3 was revealed by performing an XRD measurement. Fig. 5 shows the XRD curve of the Fe_2O_3 fragments deposited on a piece of glass. The wide peak between 18 and 38 degrees in the Figure can be due to the glass slide. However, the Figure shows clearly that the Fe_2O_3 Nano-fragments under study have an amorphous structure.

The nonlinear properties of Fe_2O_3 Nano-fragments were investigated by sing the SSPM technique with three wavelengths (405, 532, and 650 nm). At the wavelength 405 nm, concentric rings are formed with a relatively large number, as shown in Fig. 6.

At the beginning of shining the laser beam on the sample (at 0 sec), no rings appear. After a very short period (about 0.017 sec), the rings begin to form with an increasing number. They reach the maximum number after about 0.183 sec. After that, the upper part of the rings begins to shrink gradually until the rings settle in a form of approximately a half circle after the passage of (0.4 sec). The reason for the contraction of

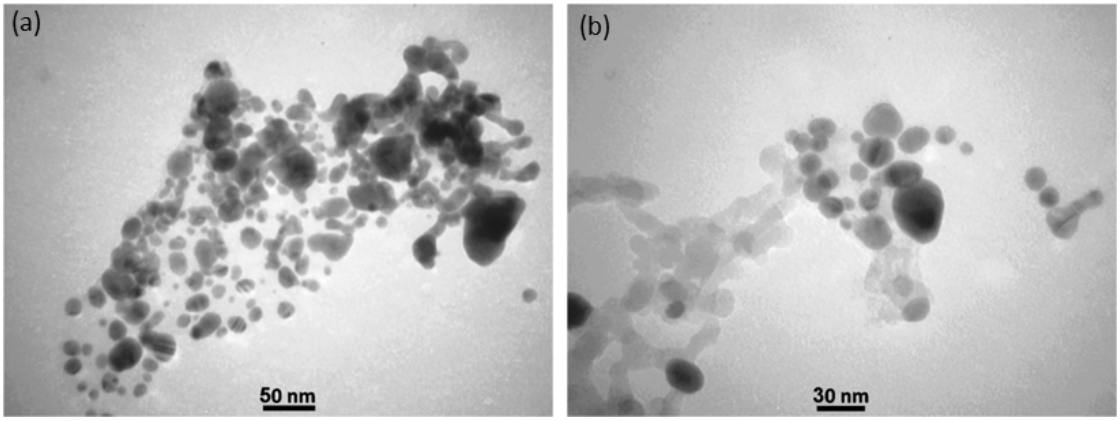

Fig. 4. TEM images for Fe_2O_3 Nano-fragments in ethanol, (a) 50 nm scale and (b) 30 nm scale

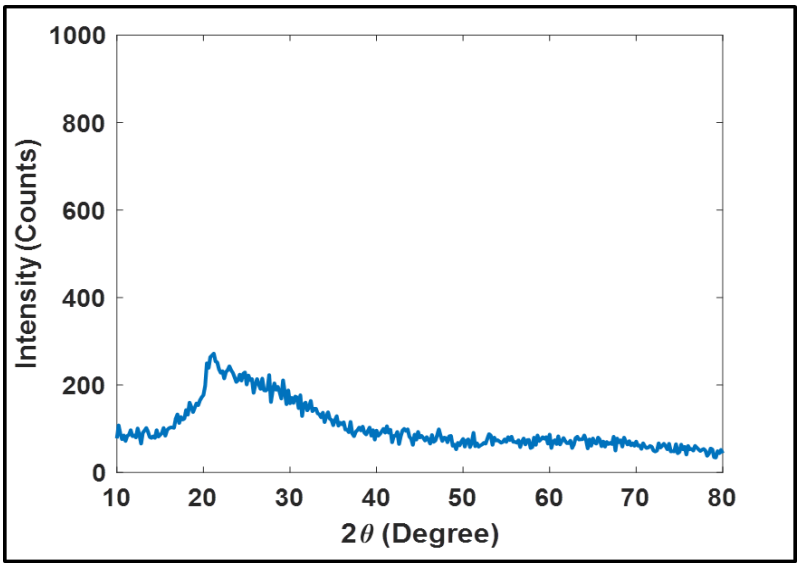

Fig. 5. XRD curve of Fe_2O_3 Nano-fragments deposited on a piece of glass

the rings is the gravity that causes irregular thermal distribution below and above the rings, as explained in [7]. The values of the nonlinear refractive index and the third-order nonlinear susceptibility calculated from the number of rings for different concentrations of Fe_2O_3 Nano-fragments are listed in Table 1.

The level of of the Fe_2O_3 particles reveals the thermal origin of this nonlinearity. In other words, the nonlinear refraction, in this case, is a result of the heat dissipated to ethanol from the Nano-fragments which, in the first place, absorbed

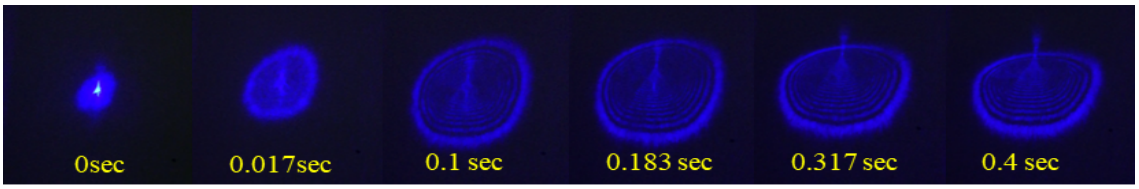

Fig. 6. The formation of diffraction rings at 405 nm from Fe_2O_3 Nano-fragments in ethanol with concentration of 0.2 mg/mL

Table 1. The Nonlinear refractive index and of Fe_2O_3 Nano-fragments in ethanol of different concentrations with 405 nm excitation wavelength.

Concentration (mg/mL)	$n_2 \times 10^{-11}$ m²/W	$\chi^{(3)}_{total} \times 10^{-8}$ e.s.u.
0.025	0.8	3.32
0.05	1.44	4.3
0.1	1.93	5.15
0.2	2.73	8.72

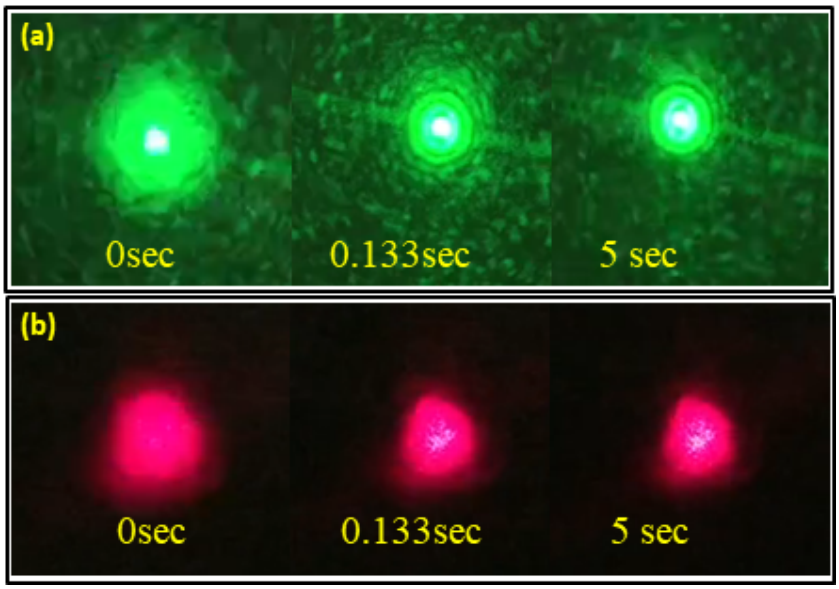

Fig. 7. The shape of the laser beam at wavelengths (a) 532 nm and (b) at 650 nm after passing through the sample cell at different times

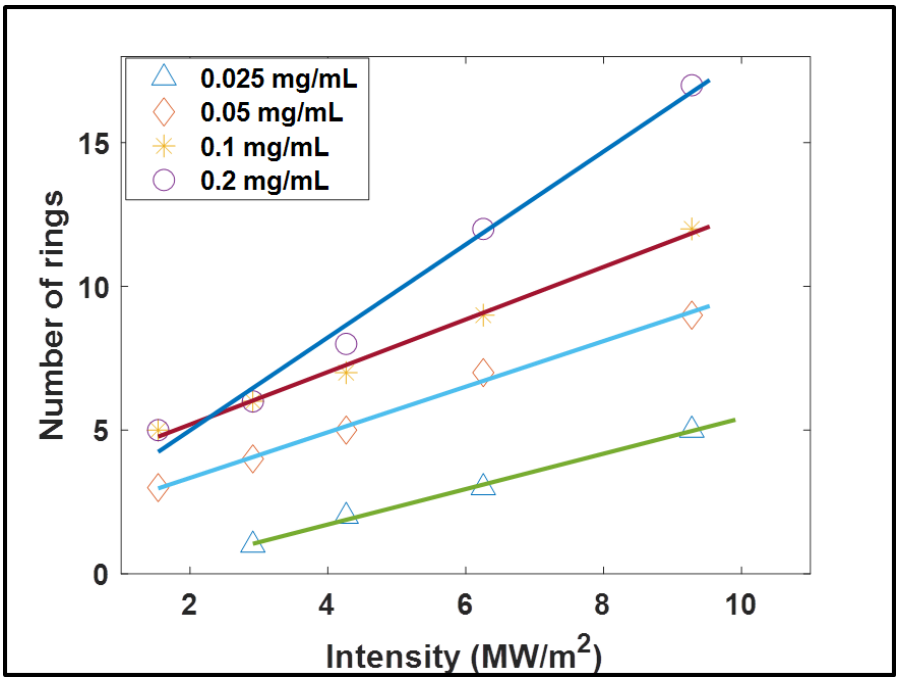

Fig. 8. The variation of rings number with the applied intensity at 405 nm for Fe_2O_3 Nano-fragments in ethanol

the incident laser radiation. The temperature distribution in such a case follows the profile of the laser beam, thus, causing unequal phase shift across the beam. This results in the formation of the diffraction rings in the far field. In addition, we note that the values of the refractive index and increase with the increase of the concentration of Nano-materials in the liquid. At wavelengths (532 and 650 nm), despite the high power of the laser used in the experiment, no rings appeared, as

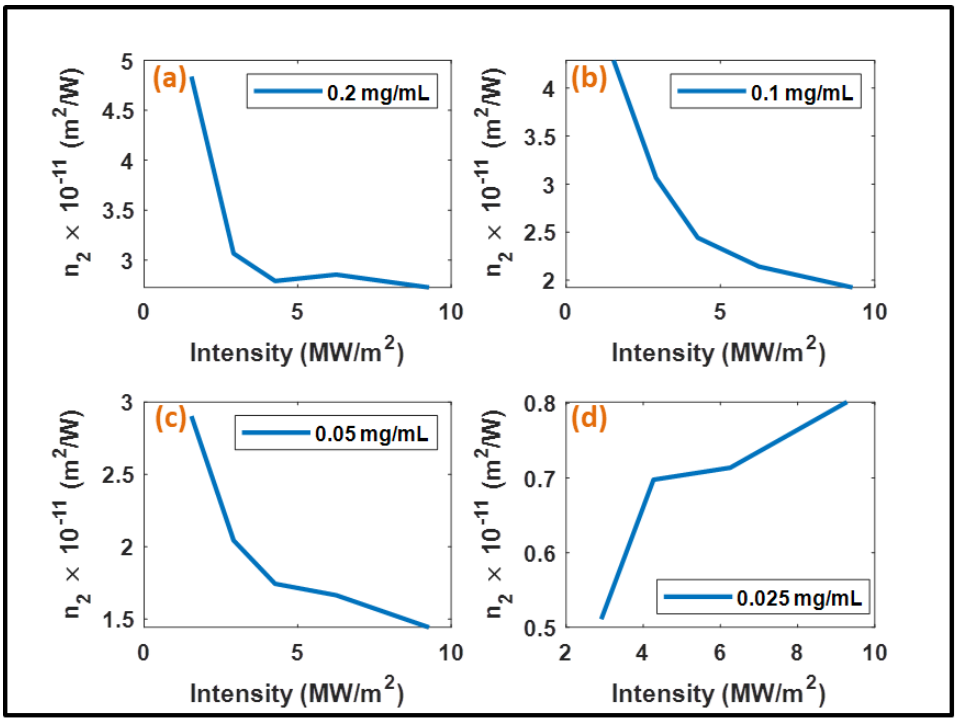

Fig. 9. Nonlinear refractive index change with incident intensity at 405nm for Fe_2O_3 Nano-fragments of concentration (a) 0.2, (b) 0.1, (c) 0.05, and (d) 0.025 mg/mL in ethanol

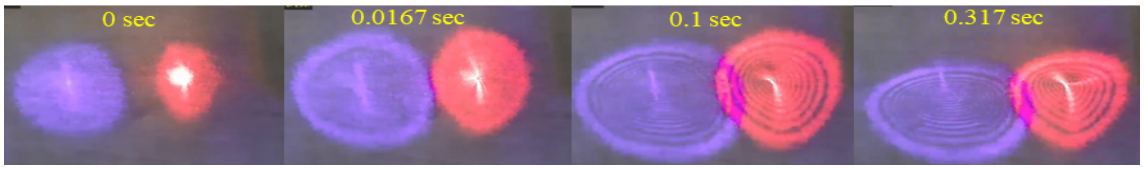

Fig. 10. Rings formation with pump beam at 405 nm and probe beam at 632.8 nm for Fe_2O_3

shown in Figs. 7 a and b, which were recorded using laser beams at 532 and 650 nm, respectively. This means that, at these wavelengths, the maximum intensity used in this work (about 25 MW/m²) is less than the threshold intensity required for the formation of the rings.

Returning to the wavelength 405 nm, to show the effect of the laser intensity, we recorded the number of rings formed at different light intensities for all concentrations under study. The result of this experiment is shown in Fig. 8.

We notice from the Figure that at wavelength 405 nm, the number of rings increases linearly with the amount of light intensity used. This linear increase is at all concentrations under study. However, despite this linear increase, the nonlinear refractive index does not change linearly with the change of the optical intensity used; but rather, its change depends on the concentration of the nanoparticle, as shown in Fig. 9.

Figs. 9 a, b, and c show that at the high concentrations (0. 2, 0.1, and 0.05 mg/mL), the value of the nonlinear refractive index decreases with the increase in the optical intensity used. This can be due to the saturation of the nonlinearity of the Nano-material, meaning that the value of the nonlinear refractive index at these concentrations is at its maximum. As for that at the lowest concentration (0.025 mg/mL), the value of the nonlinear refractive index increases slightly with the increase of the intensity of the laser used, as shown in Fig. 9d.

To design an all-optical switch, the beam at the wavelength 405 nm was used as a pump beam, and a low-intensity beam of He-Ne laser was used as a probe. When appropriate pump intensity is used, the controlling laser can induce nonlinear optical effects through the formation of diffraction rings as described above. On the other hand, the low-intensity He-Ne laser alone cannot produce any rings. However, when the pump beam is present, the diffraction rings at this wavelength and the wavelength of the probe beam are formed, as shown in Fig. 10.

In other words, the results of this experiment reveal the possibility of modifying the light of low intensity with the light of high intensity through a process based on cross-phase modulation (XPM). In this kind of process, the high-intensity laser beam works to modify the nonlinear optical properties of the medium for itself and the weak signal passing in the same medium. This leads to the generation of diffraction rings from both beams. The time evolution of the probe rings is in line with the evolution of the pump rings, as can be seen in Fig. 10. This is another proof that the basis for the excitation of the nonlinearity of the material is the high-intensity beam. These results show the possibility of using iron oxide Nano-fragments to design an optical switch that can work in different fields.

At the wavelengths 532 and 650 nm, we have previously shown that it is not possible to form diffraction rings in iron oxide Nano-fragments by using an optical intensity exceeding (25MW/m^2). This indicates that within the limits of the optical intensity used in this work, iron Nano-fragments in ethanol cannot be used to design an optical switch at these wavelengths.

CONCLUSION

Changing the environment of the Fe_2O_3 particles, from water to ethanol, led to the formation of irregular fragments with sizes ranging from 5 to 50 nm. The linear optical properties indicate a high absorbance of the Fe_2O_3 Nano-fragments in the ultraviolet region and the beginning of the visible range. By using the technique of Spatial-self-phase modulation (SSPM), it was found that these amorphous fragments in ethanol have a nonlinear refractive index of more than (m^2/W) at the wavelength of 405 nm. However, it was not possible to form diffraction rings at the two wavelengths 532 and 650 nm with light intensity exceeding 25 MW/m^2. The time for the formation of the rings from the beginning of the formation until the stability of the shape of the rings does not exceed (0.4 sec). It was also found that the value of the nonlinear refractive index, and its variation with the applied intensity, depends on the concentration of suspensions. In addition, the results indicate the possibility of designing an optical switch using Fe_2O_3 Nano-fragments at wavelength of 405 nm.

CONFLICT OF INTEREST

The authors declare that there is no conflict of interests regarding the publication of this manuscript.

REFERENCES

1. Raneesh B, Rejeena I, Rehana PU, Radhakrishnan P, Saha A, Kalarikkal N. Nonlinear optical absorption studies of sol–gel derived Yttrium Iron Garnet ($Y_3Fe_5O_{12}$) nanoparticles by Z-scan technique. Ceram Int. 2012;38(3):1823-1826.
2. Xu D, Guo Z, Tu Y, Li X, Chen Y, Chen Z, et al. Controllable nonlinear optical properties of different-sized iron phosphorus trichalcogenide ($FePS_3$) nanosheets. Nanophotonics. 2020;9(15):4555-4564.
3. Xiao S, Ma Y, He Y, Wang Y, Xin H, Fan Q, et al. Revealing the intrinsic nonlinear optical response of a single MoS_2 nanosheet in a suspension based on spatial self-phase modulation. Photonics Research. 2020;8(11):1725.
4. Majeed HA, Sharba AB. Environment-Induced Effects on The Nonlinear Refractive Index of Methyl Orange at Different Spectral Regions. Journal of Physics: Conference Series. 2021;1818(1):012131.
5. Zidan MD, El-Daher MS, Al-Ktaifani MM, Allahham A, Ghanem A. Spatial phase modulation and all-optical switching of tris(2`,2-bipyridyl)iron(II) tetrafluoroborate. Optik. 2020;219:165275.
6. Sharba AB, Ahmed RT, Haddawi SF. A comprehensive linear and nonlinear study on a fluorescent stain. Journal of Nonlinear Optical Physics & Materials. 2022;31(04).
7. Li J, Zhang Z, Yi J, Miao L, Huang J, Zhang J, et al. Broadband spatial self-phase modulation and ultrafast response of MXene $Ti_3C_2T_x$ (T=O, OH or F). Nanophotonics. 2020;9(8):2415-2424.
8. Wu L, Xie Z, Lu L, Zhao J, Wang Y, Jiang X, et al. Few-Layer Tin Sulfide: A Promising Black-Phosphorus-Analogue 2D Material with Exceptionally Large Nonlinear Optical Response, High Stability, and Applications in All-Optical Switching and Wavelength Conversion. Advanced Optical Materials. 2017;6(2).
9. Shan Y, Tang J, Wu L, Lu S, Dai X, Xiang Y. Spatial self-phase modulation and all-optical switching of graphene oxide dispersions. J Alloys Compd. 2019;771:900-904.
10. Halboos SH, Sharba AB. Solvent Effects on The Nonlinear Refractive Index of Bromocresol Purple at Three Excitation Wavelengths. Journal of Physics: Conference Series. 2021;1818(1):012103.
11. Jawad AJ, Salman QM, Jassim JM. Nonlinear characterization and optical switching of Acid red 27 dye. Journal of Physics:

Conference Series. 2021;1999(1):012151.
12. Tamgadge YS, Muley GG, Ganorkar RP. Z-scan studies of Sn doped CuO nano-colloidal suspension. Opt Mater. 2019;89:591-597.
13. Majles Ara MH, Dehghani Z, Sahraei R, Daneshfar A, Javadi Z, Divsar F. Diffraction patterns and nonlinear optical properties of gold nanoparticles. J Quant Spectrosc Radiat Transfer. 2012;113(5):366-372.
14. Yan S, Abhilash KP, Tang L, Yang M, Ma Y, Xia Q, et al. Research Advances of Amorphous Metal Oxides in Electrochemical Energy Storage and Conversion. Small. 2018;15(4).
15. Kogo A, Sanehira Y, Numata Y, Ikegami M, Miyasaka T. Amorphous Metal Oxide Blocking Layers for Highly Efficient Low-Temperature Brookite TiO_2-Based Perovskite Solar Cells. ACS Applied Materials & Interfaces. 2018;10(3):2224-2229.
16. Lin Z, Du C, Yan B, Yang G. Amorphous Fe_2O_3 for photocatalytic hydrogen evolution. Catalysis Science & Technology. 2019;9(20):5582-5592.
17. Liang S-X, Zhang L-C, Reichenberger S, Barcikowski S. Design and perspective of amorphous metal nanoparticles from laser synthesis and processing. Physical Chemistry Chemical Physics. 2021;23(19):11121-11154.
18. Ramazanov MA, Nuriyeva SG, Shirinova HA, Karimova AH, Nuriyev MA. Ag_2S/ZnS nanocomposites: Synthesis, structure and optical properties. Int J Mod Phys B. 2020;35(03):2150033.
19. Abadllah B, Kakhia M, Obaide A, Zetoun W. ZnS nanowires growth on two different types of substrate using simple thermal evaporation method. Int J Mod Phys B. 2020;34(26):2050231.
20. Tooba S, Kimiagar S, Zare-Dehnavi N. The synthesis and characterization of α-Fe_2O_3 nanowires decorated with ZnO nanoparticles. Int J Mod Phys B. 2022;36(06).
21. Ali A, Zafar H, Zia M, Ul Haq I, Phull AR, Ali JS, et al. Synthesis, characterization, applications, and challenges of iron oxide nanoparticles. Nanotechnology, science and applications. 2016;9:49-67.
22. Zhang X-L, Zhao X, Liu Z-B, Shi S, Zhou W-Y, Tian J-G, et al. Nonlinear optical and optical limiting properties of graphene oxide–Fe_3O_4 hybrid material. Journal of Optics. 2011;13(7):075202.
23. Nadafan M, Parishani M, Dehghani Z, Anvari JZ, Malekfar R. Third-order nonlinear optical properties of $NiFe_2O_4$ nanoparticles by Z-scan technique. Optik. 2017;144:672-678.
24. Chatzikyriakos G, Iliopoulos K, Bakandritsos A, Couris S. Nonlinear optical properties of aqueous dispersions of ferromagnetic γ-Fe_2O_3 nanoparticles. Chem Phys Lett. 2010;493(4-6):314-318.
25. Erken O. Effect of cycle numbers on the structural, linear and nonlinear optical properties in Fe_2O_3 thin films deposited by SILAR method. Current Applied Physics. 2022;34:7-18.
26. Sheik-Bahae M, Said AA, Wei TH, Hagan DJ, Van Stryland EW. Sensitive measurement of optical nonlinearities using a single beam. IEEE J Quantum Electron. 1990;26(4):760-769.
27. Sheik-bahae M, Said AA, Van Stryland EW. High-sensitivity, single-beam n_2 measurements. Opt Lett. 1989;14(17):955.
28. Xiao S, Lv B, Wu L, Zhu M, He J, Tao S. Dynamic self-diffraction in MoS_2 nanoflake solutions. Opt Express. 2015;23(5):5875.
29. Xiao S, Zhang Y, Ma Y, Wang Y, He Y, Zhang J, et al. Observation of spatial self-phase modulation induced via two competing mechanisms. Opt Lett. 2020;45(10):2850.
30. de Araújo CB, Gomes ASL, Boudebs G. Techniques for nonlinear optical characterization of materials: a review. Rep Prog Phys. 2016;79(3):036401.
31. Wang Y, Ren J, Zhang W, He L, Zhang X. Topologically protected long-range coherent energy transfer. Photonics Research. 2020;8(11):B39.
32. Sobhanardakani S, Jafari A, Zandipak R, Meidanchi A. Removal of heavy metal (Hg(II) and Cr(VI)) ions from aqueous solutions using Fe_2O_3@SiO_2 thin films as a novel adsorbent. Process Saf Environ Prot. 2018;120:348-357.